ISSN 1070-3632, Russian Journal of General Chemistry, 2015, Vol. 85, No. 10, pp. 2338–2347. © Pleiades Publishing, Ltd., 2015.
Original Russian Text © A.S. Burlov, S.A. Mashchenko, V.G. Vlasenko, E.D. Garnovskaya, Ya.V. Zubavichus, S.I. Levchenkov, Yu.S. Kurinnaya, 2015, published in Zhurnal Obshchei Khimii, 2015, Vol. 85, No. 10, pp. 1708–1717.

Chemical and Electrochemical Synthesis, Local Atomic Structure, and Properties of Copper(II), Cobalt(II), and Nickel(II) Complexes with Azo Compounds Containing an Additional Azo Group in the *para* or *ortho* Position of the Amine Fragment

A. S. Burlov[a], **S. A. Mashchenko**[a], **V. G. Vlasenko**[b], **E. D. Garnovskaya**[a], **Ya. V. Zubavichus**[c],
S. I. Levchenkov[d], **and Yu. S. Kurinnaya**[a]

[a] *Research Institute of Physical and Organic Chemistry, Southern Federal University,*
pr. Stachki 194/2, Rostov-on-Don, 344090 Russia
e-mail: anatoly.burlov@yandex.ru

[b] *Research Institute of Physics, Southern Federal University,*
pr. Stachki 194, Rostov-on-Don, 344090 Russia

[c] *"Kurchatov Institute" National Research Center, pl. Akademika Kurchatova 1, Moscow, 123182 Russia*

[d] *Southern Scientific Center, Russian Academy of Sciences, ul. Chekhova 41, Rostov-on-Don, 344006 Russia*

Received May 18, 2015

Abstract—New copper(II), cobalt(II), and nickel(II) complexes with 1-[4-(phenydiazenyl)phenyldiazenyl]-naphthalen-2-ol and 1-[4-methyl-2-(4-methylphenyldiazenyl)phenyldiazenyl]naphthalen-2-ol have been synthesized by chemical and electrochemical methods and characterized by IR, ^{1}H NMR, and X-ray absorption spectroscopy, as well as by magnetochemistry and quantum chemical calculations. Coordination of the nitrogen atom in the additional azo group to the metal ion is determined by its position (*ortho* or *para*) and metal nature.

Keywords: azo compounds, metal chelates, X-ray absorption spectroscopy, local atomic structure, magnetochemistry, quantum chemical calculations

DOI: 10.1134/S1070363215100199

Aromatic and heterocyclic azo ligands and metal complexes derived therefrom are the most important targets of modern coordination chemistry [1–3]. They constitute the most significant class of organic dyes [4] and are widely used in fundamental and applied studies as components of electrochromic materials and modern data recording and storage devices [1], as well as in many biological reactions [5, 6] and analytical chemistry [7, 8]. Photochromic molecules promising for the design of polyfunctional materials have been obtained on their basis [1, 9–13]. Furthermore, azo compounds are interesting as ligand systems for studying intrachelate competitive coordination [14–16].

If an azo complex molecule contains an additional azo group which may be involved in the coordination or not, it may undergo photoinduced *E*/*Z*-isomerization; such coordination compounds are promising for the design of molecular switches and photoactive materials [17–21].

In continuation of our previous studies [17, 18, 22, 23], in the present work we have synthesized Cu(II), Co(II), and Ni(II) coordination compounds **3** and **4** with 1-[4-(phenyldiazenyl)phenyldiazenyl]naphthalen-2-ol (**1**) and 1-[4-methyl-2-(4-methylphenyldiazenyl)-phenyldiazenyl]naphthalen-2-ol (**2**) by chemical and electrochemical methods (Scheme 1). The structure of complexes **3** and **4** was determined by elemental analysis, magnetochemistry, and IR, ^{1}H NMR, and X-ray absorption spectroscopy.

According to the IR and ^{1}H NMR data, ligands **1** and **2** in solution exist as azo tautomers. This follows from the presence of OH proton signals in their ^{1}H

Scheme 1.

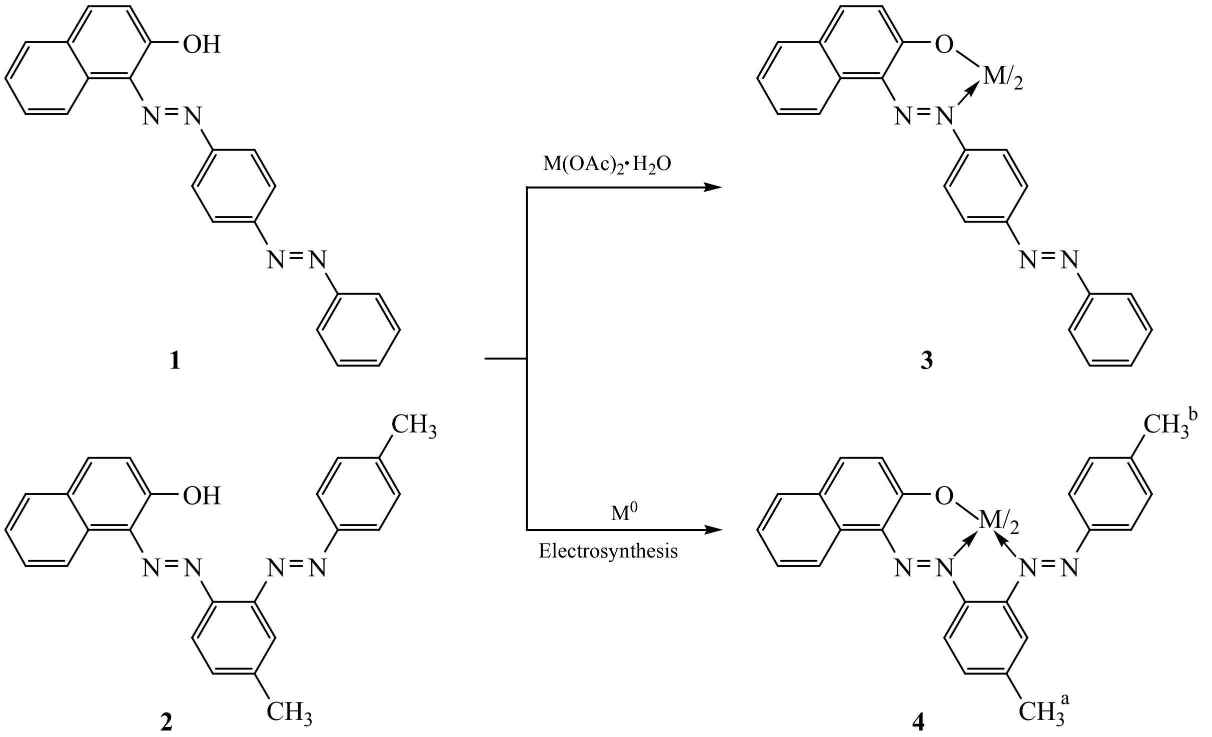

M = Cu (**a**), Co (**b**), Ni (**c**).

NMR spectra at δ 16.34 and 17.13 ppm, respectively. The IR spectra of **1** and **2** displayed absorption bands due to OH stretching vibrations at 3038 and 3022 cm^{-1}. In going from the free ligands to their complexes **3** and **4**, the OH band disappears from the IR spectra, indicating deprotonation of the ligand.

In keeping with the elemental analyses, complexes **3** and **4** obtained by both chemical and electrochemical methods have the composition ML_2. The electrochemical procedure ensured a higher yield of the complexes (by 10–15%).

Copper and cobalt complexes **3a**, **3b**, **4a**, and **4b** and nickel complex **4c** are paramagnetic; the μ_{ef} values are 1.85–1.97 (Cu), 4.11–3.94 (Co), and 3.06 B.M. (**4c**) at 274 K, and they do not change as the temperature decreases. This indicates that the complexes are monomeric. Nickel complex **3c** is diamagnetic at 274 K.

We failed to obtain single crystals of **3** and **4** suitable for X-ray analysis. Therefore, local atomic environment of metal ions in chelates **3** and **4** was studied by X-ray absorption spectroscopy (XANES/EXAFS).

Figures 1–3 show XANES and Fourier-transformed EXAFS Cu, Co, and Ni *K*-edges for compounds **3** and **4**. The inserts in Figs. 1–3 show XANES pre-edge regions and the corresponding first derivatives. It is seen that that the intensity of XANES pre-edge peaks A strongly depends on the atom nature. It is well known [24] that pre-edge peaks arise from $1s\rightarrow3d$ electronic transitions and their intensity I^A is determined by the population of the vacant *d*-orbital of the metal ($I_{Co} > I_{Ni} > I_{Cu}$). In addition, pre-edge peak intensity strongly depends on the symmetry of the nearest environment of the metal in a complex. Pre-edge peaks are the most intense when the metal environment geometry lacks an inversion center, e.g., in tetrahedral configuration; symmetric octahedral or square geometry is characterized by a low-intense pre-edge peak. This is related to the reduction of *p*–*d*-mixing of metal orbitals in going to more symmetric environment. The degree of symmetry is also reflected in the near-edge shape, which can be clearly seen from the shape of the first derivative. The octahedral environment features degeneracy of the vacant *p* states involved in electronic transitions responsible for the absorption *K*-edge; in this case, the first derivative of the edge profile displays a strong narrow maximum.

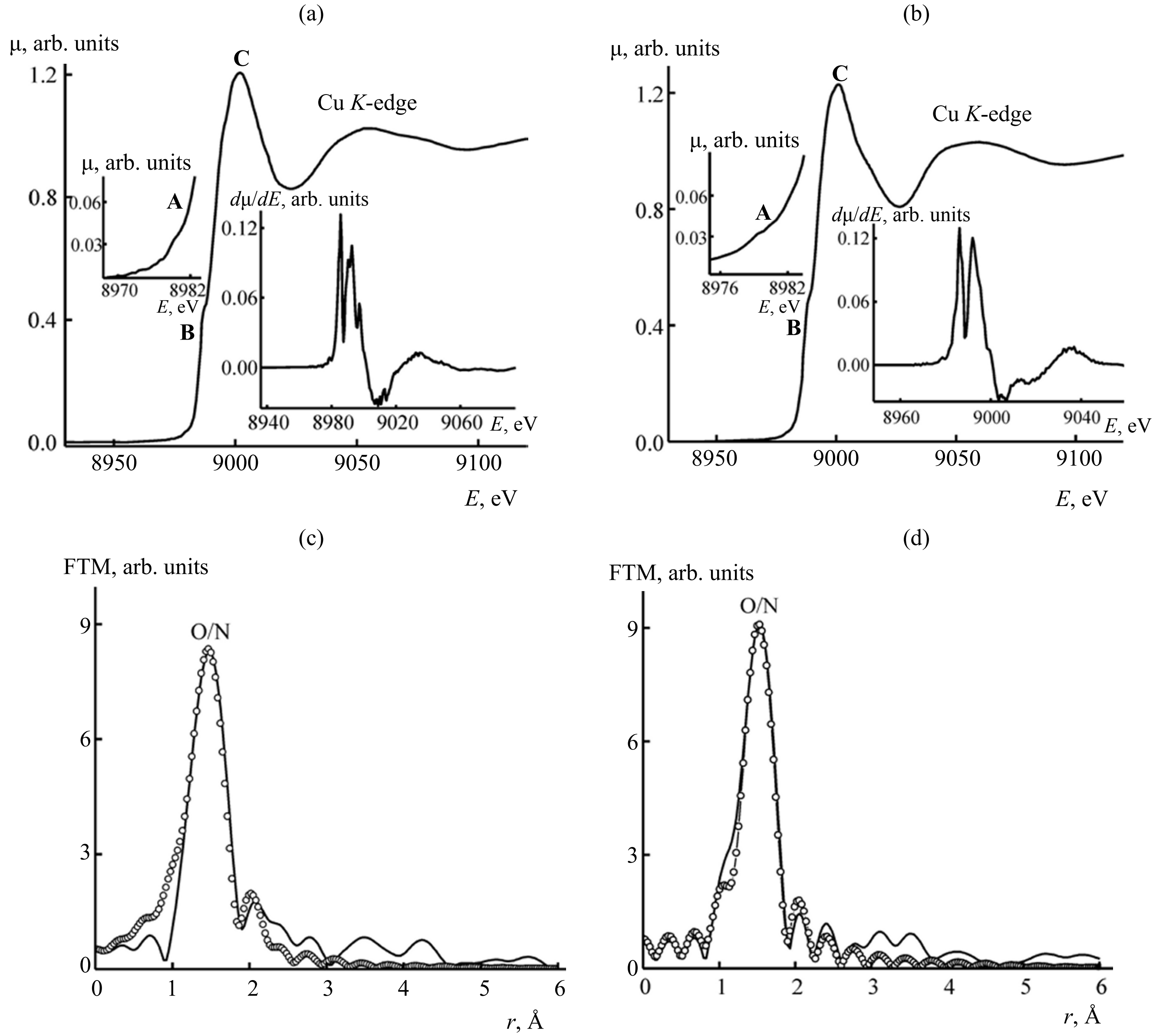

Fig. 1. (a, b) XANES and (c, d) EXAFS Fourier transform magnitude (FTM) Cu *K*-edge spectra of complexes (a, c) **3a** and (b, d) **4a**. Experimental curves are shown with solid lines, and calculated curves, with circles). Hereinafter, the XANES pre-edge region and the first derivative of the edge are shown in the inserts.

There is no such MO degeneracy in tetrahedral or square environment, and the maximum of the first derivative of the edge is broadened or several maxima may appear.

The XANES Cu *K*-edge spectra of **3a** and **4a** (Fig. 1) showed low-intense pre-edge peak (**A**) intensities and almost similar shapes of the first derivatives, which indicated similar geometries of the coordination entities in these complexes. The low intensity of pre-edge peak **A** in combination with the presence of a shoulder (**B**) (which is observed in the spectra of the square planar complexes due to $1s \rightarrow 4p_z$ electronic transitions, where the *z* axis is orthogonal to the square plane) corresponds to the square–planar environment of copper(II) ions in these complexes, regardless of the position of the additional azo group.

Substantially different patterns were observed in the XANES Co *K*-edge spectra of **3b** and **4b** (Fig. 2). The pre-edge peak intensity of **3b** (*para*-phenylazo ligand) is considerably higher than that observed for *ortho*-

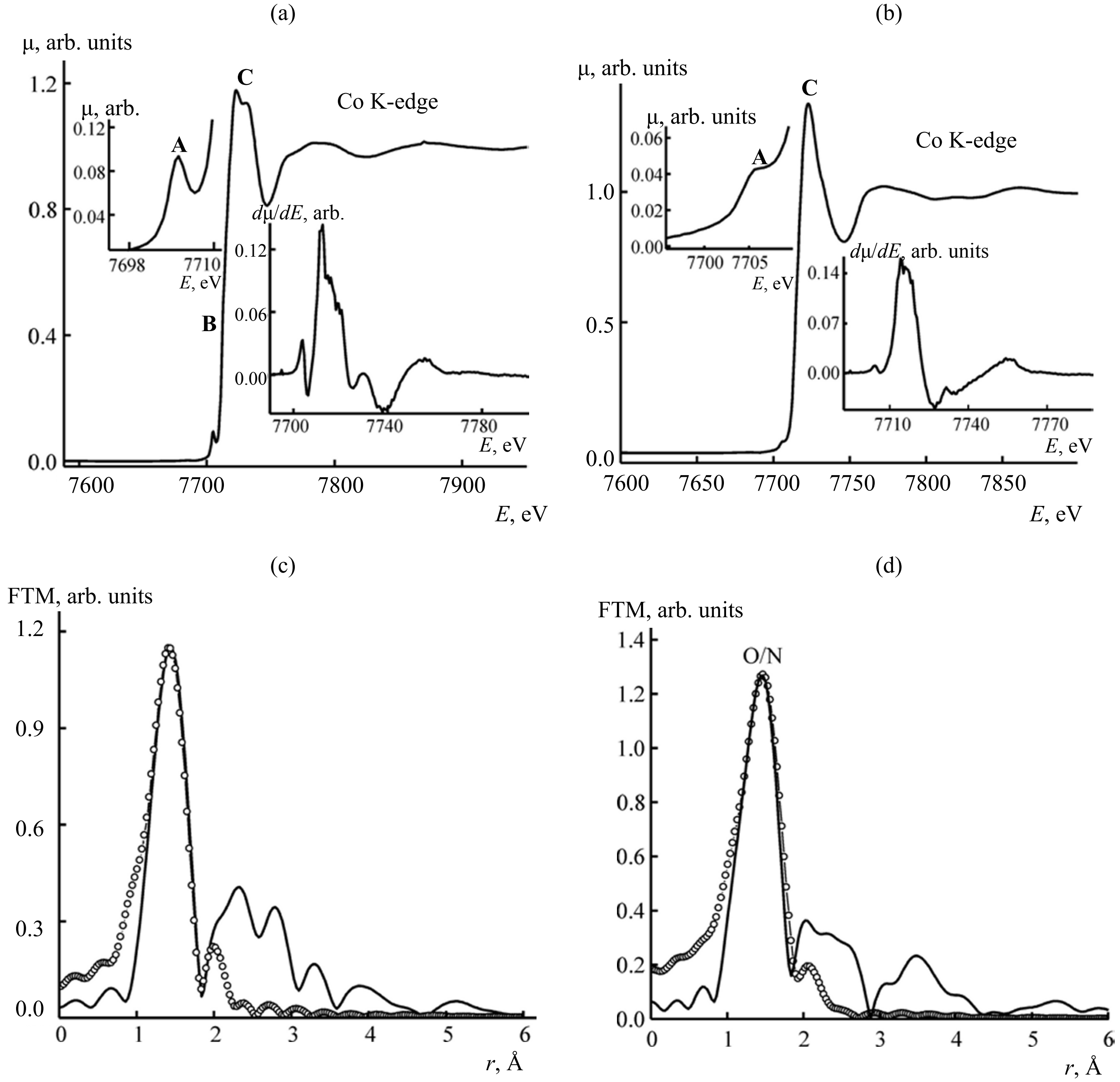

Fig. 2. (a, b) XANES and (c, d) EXAFS Fourier transform magnitude Cu *K*-edge spectra of complexes (a, c) **3b** and (b, d) **4b**. Experimental curves are shown with solid lines, and calculated curves, with circles).

substituted analog **4b**. The first derivative of the edge profile of **3b** features several maxima in contrast to the narrow maximum on the first derivative for **4b**. Furthermore, the Co *K*-edge of **4b** lacks shoulder **B**, and the main absorption maximum (**C**) contributed mainly by $1s \rightarrow 4p_{xy}$ electronic transitions appears as a narrow peak; the corresponding maximum for **3b** is split. These qualitative differences allowed us to conclude that the coordination environment of the cobalt ion in **4b** is more symmetric than in **3b**. The higher symmetry may be achieved via additional coordination of the nitrogen atom in the *ortho* position. The set of XANES parameters of **3b** suggests tetrahedral environment of the cobalt atom in this complex.

The XANES Ni *K*-edge spectrum of **3c** (*para*-phenylazo) characteristically displayed maximum **B** (see above for copper complexes) which clearly indicates square–planar coordination entity. This is also confirmed by splitting of the first derivative into

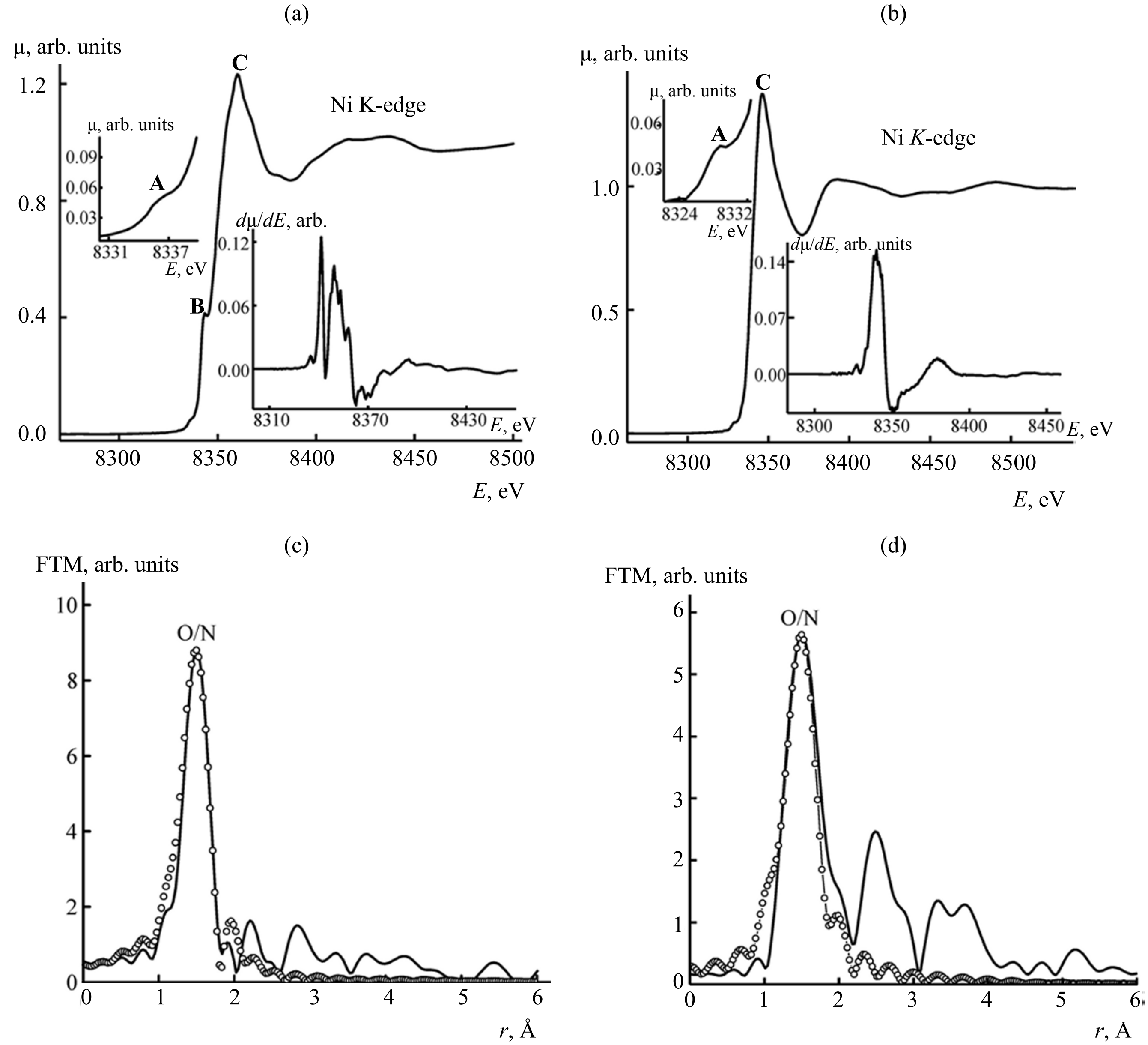

Fig. 3. (a, b) XANES and (c, d) EXAFS Fourier transform magnitude Cu *K*-edge spectra of complexes (a, c) **3c** and (b, d) **4c**. Experimental curves are shown with solid lines, and calculated curves, with circles).

several maxima and low intensity of pre-edge peak **A**. The XANES Ni *K*-edge spectrum of **4c** (*ortho* analog) resembles the Co *K*-edge spectrum of **4b**, so that additional coordination of nitrogen with formation of pseudooctahedral coordination entity may be assumed for **4c**.

Quantitative characteristics of the nearest environment of metal ions in complexes **3** and **4** were obtained from the EXAFS spectra. Several geometries of coordination entities therein were considered. The results of simulation of the first coordination sphere are collected in table (local structure parameters for models with the lowest *Q* values are given).

Thus, XANES analysis showed the best model of local atomic structure of copper complexes **3a** and **4a** implies square–planar coordination entity with almost equal Cu···N and Cu···O distances (1.95 Å).

EXAFS data analysis revealed substantially different local atomic structure of cobalt complexes **3b** and **4b**. The first coordination sphere of **3b** includes

Local atomic structure parameters of metal chelates **3a**–**3c** and **4a**–**4c** obtained by analysis of EXAFS Cu, Co, and Ni *K*-edges[a]

Compound no.	*N*	*R*, Å	σ^2, Å^2	Coordination sphere	*Q*, %
3a	4	1.95 (2×1.868, 2×2.007)	0.0045	N/O	1.1
4a	4	1.95 (2×1.916, 1.979, 2.002)	0.0035	N/O	1.5
	6	1.97	0.0056	N/O	2.1
	4	1.94	0.0035	N/O	1.6
	2	2.01	0.0035	N/O	
3b	4	1.93 (2×1.822, 2×1.909)	0.0058	N/O	4.2
4b	4	2.00	0.0034	N/O	4.1
	6	2.03	0.0096	N/O	1.4
	4	1.98	0.0076	N/O	0.1
	2	2.05 (1.897, 1.900, 1.948, 1.930, 1.877, 1.888)	0.0059	N/O	
3c	2	1.86 (2×1.823)	0.0036	N/O	2.2
	2	1.91 (2×1.892)	0.0036	N/O	
	2	1.93	0.0030	N/O	3.5
4c	2	2.01	0.0030	N/O	
	4	2.00	0.0030	N/O	0.2
	2	2.11 (2.024, 2.009, 2.040, 2.052, 1.871, 1.885)	0.0060	N	

[a] *R* is the interatomic distance, *N* is the coordination number, σ^2 is the Debye–Waller factor, and *Q* is the goodness of fit. Calculated interatomic distances are given in parentheses.

four nitrogen and oxygen atoms, and its average radius is about 1.93 Å. With account taken of the XANES data, tetrahedral environment of the cobalt atom in **3b** can be presumed. The best model of **4b** conforms to a distorted octahedral environment of Co in keeping with the conclusions drawn by XANES analysis.

As follows from the XANES and EXAFS data for nickel complexes **3c** and **4c**, *ortho* position of the second azo group the latter enables additional coordination of its nitrogen atom. The local atomic structure of **4c** corresponds to the octahedral environment of nickel ion where two Ni···N or Ni···O distances are longer than the other two. However, unlike cobalt complex **3b**, complex **3c** features square–planar coordination mode with average distances *R* of 1.89 Å.

The geometric structures and interatomic distances in the coordination entities of complexes **3** and **4**, determined by quantum chemical calculations with full geometry optimization, showed a good agreement with the data of X-ray absorption spectroscopy. The optimized structures of molecules **3a** and **4c** as examples are shown in Fig. 4, and the calculated interatomic distances are compared to the experimental coordination sphere radii in table. It is seen that the differences for the first coordination sphere amount to ~0.02 Å, which is within the error of the X-ray spectroscopic method.

In summary, by XANES and EXAFS data analysis and quantum chemical calculations we have shown that complexes **4b** and **4c** derived from *ortho*-bis-azo ligand **2** are characterized by octahedral coordination due to additional N→M dative bonds. Analogous interaction in complexes **3b** and **3c** with *para*-bis-azo ligand **1** is hindered for steric reasons, and the coordination mode in these complexes is close to tetrahedral. Copper complexes **3a** and **4a** have square–planar coordination entity, regardless of the ligand structure.

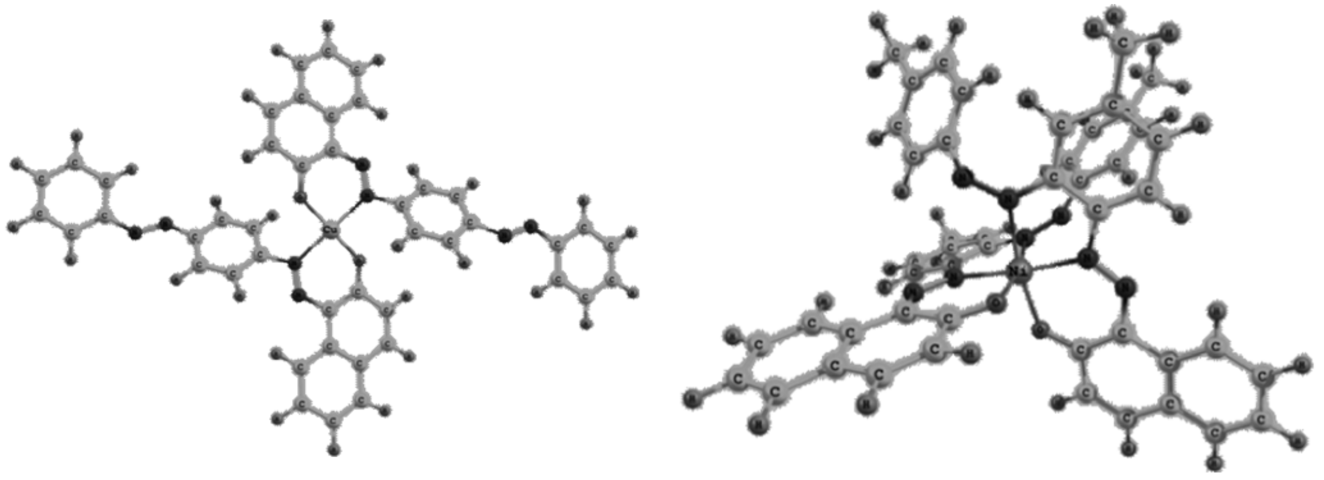

Fig. 4. Optimized structures of molecules **3a** and **4c** according to DFT B3LYP/6-31G(*d*) calculations.

EXPERIMENTAL

The IR spectra (ATR) were recorded on a Varian Excalibur–3100 FT-IR spectrometer from powdered samples. The ^{1}H NMR spectra were measured on a Varian Unity-300 instrument (300 MHz; internal stabilization by ^{2}H in $CDCl_3$). The XANES spectra were obtained in the transmission mode on an EXAFS spectrometer at the Structural Materials Science end-station (Kurchatov Center for Synchrotron Radiation and Nanotechnology, Moscow) [25]; electron beam energy 2.5 GeV, current 80–100 mA; double-crystal Si(111) monochromator.

The X-ray absorption spectra were processed by standard procedures, including background subtraction, normalization to the *K*-edge jump, and isolation of atomic absorption μ_0 [26], followed by Fourier transform of the EXAFS (χ) spectra in the range of photoelectron wave vectors k from 2.6 to 12–13 Å^{-1} with a weight function k^3. The resulting Fourier transformed χ-spectra corresponded within the phase shift to the radial distribution function of atoms nearest to the absorbing metal atom. The threshold ionization energy E_0 was set at the maximum of the first derivative of the *K*-edge and was then varied during the fitting procedure.

The precise structural parameters of the nearest environment of the metal atoms in the complexes were determined by nonlinear fitting of the corresponding coordination spheres (by comparing the calculated EXAFS signals with that isolated by Fourier filtration from the total EXAFS spectrum) using IFFEFIT package [27]. The phases and amplitudes of photoelectron scattering necessary for the model spectrum were calculated with the aid of FEFF7 [28]. The initial coordinates of atoms for the calculation of scattering phase shifts and amplitudes and subsequent fitting were taken from the X-ray diffraction data for structurally related metal complexes available from the Cambridge Structural Database [29].

The goodness-of-fit function Q was calculated by the formula

$$Q(\%) = \frac{\Sigma[k\chi_{\exp}(k) - k\chi_{th}(k)]^2}{\Sigma[k\chi_{\exp}(k)]^2} \times 100\%.$$

Minimization of Q was performed to determine structural parameters of the nearest environment of metal ions.

The specific magnetic susceptibilities of solid samples were determined by the Faraday method in the temperature range 77.4–300 K using $Hg[Co(CNS)_4]$ as calibration standard.

DFT quantum chemical calculations of the complexes in the ground state were performed using GAUSSIAN 03 package [30] with the B3LYP three-parameter hybrid functional [31, 32] and 6-31G(*d*) standard split-valence polarization basis set [33]. This calculation method was repeatedly used previously to optimize molecular structures of both organic and metal coordination compounds.

Naphthalen-2-ol, 4-(phenyldiazenyl)aniline, and 4-methyl-2-(4-methylphenyldiazenyl)aniline were commercial products.

Azo compounds **1** and **2** were synthesized by diazotization of 1.97 g (0.01 mol) of 4-(phenyldiazenyl)aniline or 2.25 g (0.01 mol) of 4-methyl-2-(4-methylphenyldiazenyl)aniline, followed by azo coupling with 1.44 g (0.01 mol) of naphthalen-2-ol in 40 mL of ethanol [34]. The products were recrystallized from DMF–propan-2-ol (1 : 2).

1-[4-(Phenyldiazenyl)phenyldiazenyl]naphthalen-2-ol (1). Yield 65%, red powder, mp 190–191°C. IR spectrum, ν, cm^{-1}: 3038 (OH), 1416, 1392 (N=N), 1301 (C$_{\text{arom}}$–O). ^{1}H NMR spectrum (CDCl$_3$), δ, ppm: 6.76–8.52 m (15H, H$_{\text{arom}}$), 16.34 s (1H, OH). Found, %: C 74.87; H 4.49; N 15.97. $C_{22}H_{16}N_4O$. Calculated, %: C 74.98; H 4.58; N 15.90.

1-[4-Methyl-2-(4-methylphenyldiazenyl)phenyldiazenyl]naphthalen-2-ol (2). Yield 60%, red crystals, mp 160–161°C. IR spectrum, ν, cm^{-1}: 3024 (OH), 1421, 1395 (N=N), 1306 (C$_{\text{arom}}$–O). ^{1}H NMR spectrum (CDCl$_3$), δ, ppm: 2.41 s (3H, CH$_3^a$), 2.43 s (3H, CH$_3^b$), 6.73–8.49 m (13H, H$_{\text{arom}}$), 17.13 s (1H, OH). Found, %: C 75.69; H 5.36; N 14.79. $C_{24}H_{20}N_4O$. Calculated, %: C 75.77; H 5.30; N 14.73.

Complexes 3 and 4 *(general procedures). a.* A solution of 0.5 mmol of copper(II), cobalt(II), or nickel(II) acetate in 10 mL of methanol was added to a solution of 1 mmol of compound **1** or **2** in 20 mL of DMF–propan-2-ol (1 : 2). The mixture was heated for 1 h under reflux and cooled, and the precipitate was filtered off, washed with methanol, and recrystallized from DMF–propan-2-ol (1 : 2).

b. An electrochemical cell equipped with a platinum cathode and copper, cobalt, or nickel anode was charged with a solution of 0.001 mol of azo compound **1** or **2** in 20 mL of DMF–propan-2-ol (1 : 2) and 0.01 g of [Et$_4$N]ClO$_4$ as supporting electrolyte. The synthesis was carried out at a current of 40 mA (15 V, 1 h). When the reaction was complete, the precipitate was filtered off, washed with methanol, and recrystallized from DMF–propan-2-ol (1 : 2).

Bis{1-[4-(phenyldiazenyl)phenyldiazenyl]naphthalen-2-olato}copper(II) (3a). Yield 76 (*a*), 87% (*b*); brown powder, mp >250°C, μ$_{\text{ef}}$ = 1.97 B.M. (294 K). IR spectrum, ν, cm^{-1}: 1403 (N=N), 1310 v.s (C$_{\text{arom}}$–O). Found, %: C 68.79; H 4.29; Cu 9.51; N 12.67 (*a*); C 68.75; H 4.22; Cu 9.49; N 12.69 (*b*). $C_{38}H_{28}CuN_6O_2$. Calculated, %: C 68.71; H 4.25; Cu 9.57; N 12.65.

Bis{1-[4-(phenyldiazenyl)phenyldiazenyl]naphthalen-2-olato}cobalt(II) (3b). Yield 87 (*a*), 97% (*b*); dark brown powder, mp >250°C, μ$_{\text{ef}}$ = 4.11 B.M. (294 K). IR spectrum, ν, cm^{-1}: 1404 (N=N), 1258, 1320 (C$_{\text{arom}}$–O). Found, %: C 69.40; H 3.93; Co 7.70; N 14.77 (*a*); C 69.46; H 3.92; Co 7.20; N 14.78 (*b*). $C_{44}H_{30}CoN_8O_2$. Calculated, %: C 69.38; H 3.97; Co 7.74; N 14.71.

Bis{1-[4-(phenyldiazenyl)phenyldiazenyl]-naphthalen-2-olato}nickel(II) (3c). Yield 81 (*a*), 96% (*b*); dark brown powder, mp >250°C; diamagnetic. IR spectrum, ν, cm^{-1}: 1406 (N=N), 1311 (C$_{\text{arom}}$–O). Found, %: C 69.47; H 3.93; N 14.75; Ni 7.69 (*a*); C 69.42; H 3.95; N 14.79; Ni 7.39 (*b*). $C_{44}H_{30}N_8NiO_2$. Calculated, %: C 69.40; H 3.97; N 14.70; Ni 7.71.

Bis{1-[4-methyl-2-(4-methylphenyldiazenyl)-phenyldiazenyl]naphthalen-2-olato}copper(II) (4a). Yield 85 (*a*), 95% (*b*); brown powder, mp >250°C, μ$_{\text{ef}}$ = 1.85 B.M. (294 K). IR spectrum, ν, cm^{-1}: 1404 (N=N), 1315 (C$_{\text{arom}}$–O). Found, %: C 70.15; H 4.71; Cu 7.75; N 13.69 (*a*); C 70.13; H 4.61; Cu 7.69; N 13.61 (*b*). $C_{48}H_{38}N_8CuO_2$. Calculated, %: C 70.10; H 4.66; Cu 7.72; N 13.63.

Bis{1-[4-methyl-2-(4-methylphenyldiazenyl)-phenyldiazenyl]naphthalen-2-olato}cobalt(II) (4b). Yield 83 (*a*), 94% (*b*); dark brown powder, mp >250°C, μ$_{\text{ef}}$ = 3.94 B.M. (294 K). IR spectrum, ν, cm^{-1}: 1405 (N=N), 1318 (C$_{\text{arom}}$–O). Found, %: C 70.47; H 4.72; Co 7.25; N 13.68 (*a*); C 70.41; H 4.76; Co 7.19; N 13.62 (*b*). $C_{48}H_{38}N_8CoO_2$. Calculated, %: C 70.50; H 4.68; Co 7.21; N 13.70.

Bis{1-[4-methyl-2-(4-methylphenyldiazenyl)-phenyldiazenyl]naphthalen-2-olato}nickel(II) (4c). Yield 88 (*a*), 98% (*b*); dark brown powder, mp >250°C, μ$_{\text{ef}}$ = 3.06 B.M. (294 K). IR spectrum, ν, cm^{-1}: 1407 (N=N), 1311 (C$_{\text{arom}}$–O). Found, %: C 70.48; H 4.71; N 13.69; Ni 7.23 (*a*); C 70.55; H 4.78; N 13.75; Ni 7.15 (*b*). $C_{48}H_{38}N_8NiO_2$. Calculated, %: C 70.52; H 4.68; N 13.71; Ni 7.18.

The IR and ^{1}H NMR spectra were recorded using the equipment of the “Molecular Spectroscopy” Joint Center at the Southern Federal University.

ACKNOWLEDGMENTS

This work was performed using the equipment of Unique Scientific Facility “Kurchatov Synchrotron Radiation Source” supported by the Russian Ministry of Science and Education (project code RFMEFI61914X0002).

This study was performed under financial support by the Russian Foundation for Basic Research (project nos. 14-03-31 419_mol_a, 13-03-00 171 a).

REFERENCES

1. *Comprehensive Coordination Chemistry II*, McCleverty, Y.A. and Meyer, T.J., Eds., Amsterdam: Elsevier, 2004.
2. Bhunia, P., Sardar, D., Sarker, K.K., Ray, U.S., Ray, J.-S., Wu, J.S., Lu, T.-H., and Sinha, C., *J. Coord. Chem*., 2009, vol. 62, p. 552. DOI: 10.1080/00958970802291282.
3. Nandi, S., Bannerjee, D., Wu, J.-S., Lu, T.-H., Slawin, A.M.Z., Woolins, J.D., Ribas, J., and Sinha, C., *Eur. J. Inorg. Chem*., 2009, no. 26, p. 3972. DOI: 10.1002/ejic.200900423.
4. Porai-Koshits, B.A., *Azokrasiteli* (Azo Dyes), Leningrad: Khimiya, 1972.
5. Kondil, S.S., *Transition Met. Chem*., 1998, vol. 23, p. 461. DOI: 10.1023/A:1006900923122.
6. Daniel, J.W., *Toxicol. Appl. Pharmacol*., 1962, vol. 4, p. 572.
7. Broekaert, J.A. and Hörmann, P.K., *Anal. Chim. Acta*, 1981, vol. 124, p. 421. DOI: 10.1016/S0003-2670(01)93591-3.
8. Kurtoglu, M., Birbicer, N., Kimyonsen, U., and Serin, S., *Dyes Pigm*., 1999, vol. 41, p. 143.
9. Sato, O., Tao, J., and Zhang, Y.-Z., *Angew. Chem. Int. Ed*., 2007, vol. 46, p. 2152. DOI: 10.1002/anie.200602205.
10. Ire, M., *Chem. Rev*., 2000, vol. 100, no. 5, p. 1683. DOI: 10.1021/cr980068l.
11. Delaire, J.A. and Nakatani, K., *Chem. Rev*., 2000, vol. 100, no. 5, p. 1817. DOI: 10.1021/cr980078m.
12. Lee, S.H., Kim, S.K., Bok, J.H., Yoon, J., Lee, K., and Kim, J.S., *Tetrahedron Lett*., 2005, vol. 46, no. 47, p. 8163. DOI: 10.1016/j.tetlet.2005.09.117.
13. Sarker, K.K., Sardar, D., Suwa, K., Otsuki, J., and Sinha, C., *Inorg. Chem*., 2007, vol. 46, no. 20, p. 8291. DOI: 10.1021/ic7012073.
14. *Synthetic Coordination and Organometallic Chemistry*, Garnovskii, A.D. and Kharisov, B.I., Eds., New York: Marcel Dekker, 2003.
15. Garnovskii, A.D. and Vasil'chenko, I.S., *Russ. Chem. Rev*., 2005, vol. 74, no. 3, p. 193. DOI: 10.1070/RC2005v074n03ABEH001164.
16. Kogan, V.A. and Shcherbakov, I.N., *Ros. Khim. Zh*., 2004, vol. 48, no. 1, p. 69.
17. Burlov, A.S., Nikolaevskii, S.A., Vasil'chenko, I.S., Koshchienko, Y.V., Uraev, A.I., Sennikova, E.V., Borodkin, G.S., Garnovskii, A.D., Minkin, V.I., Bogomyakov, A.S., Vlasenko, V.G., and Garnovskii, D.A., *Russ. J. Coord. Chem*., 2009, vol. 35, no. 7, p. 486.
18. Garnovskii, A.D., Burlov, A.S., Metelitsa, A.V., Vasil'chenko, I.S., Nikolaevskii, S.A., Borodkina, I.G., Minkin, V.I., Starikov, A.G., and Bezugliy, S.O., *Russ. J. Coord. Chem*., 2010, vol. 36, no. 7, p. 479.
19. Gütlich, P., Garcia, Y., and Wolke, T., *Coord. Chem. Rev*., 2001, vols. 219–221, p. 839. DOI: 10.1016/S0010-8545(01)00381-2.
20. Wang, P., Ming, H., Zhang, J.Y., Liang, Z.C., Lu, Y.H., Zhang, Q.J., Xie, J.P., and Tian, Y.P., *Opt. Commun*., 2002, vol. 203, p. 159. DOI: 10.1016/S0030-4018(02)01098-2
21. Weber, B., *Coord. Chem. Rev*., 2009, vol. 253, p. 2432. DOI: 10.1016/j.ccr.2008.10.002.
22. Burlov, A.S., Mashchenko, S.A., Nikolaevskii, S.A., Uraev, A.I., Korshunova, E.V., Antsyshkina, A.S., Sadikov, G.G., Sergienko, V.S., Kiskin, M.A., Vlasenko, V.G., Zubavichus, Ya.V., Garnovskii, D.A., and Levchenkov, S.I., *Russ. J. Coord. Chem*., 2013, vol. 39, no. 12, p. 813. DOI: 10.7868/S0132344X13120013.
23. Burlov, A.S, Mashchenko, S.A., Vlasenko, V.G., Zubavichus, Y.V., Uraev, A.I., Lyssenko, K.A., Levchenkov, S.I., Vasilchenko, I.S., Garnovskii, D.A., and Borodkin, G.S., *J. Mol. Struct*., 2014, vol. 1061, p. 47. DOI: 10.1016/j.molstruc.2013.12.007.
24. Yamamoto, T., *X-Ray Spectrom*., 2008, vol. 37, p. 572. DOI: 10.1002/xrs.1103.
25. Chernyshov, A.A., Veligzhanin, A.A., and Zubavichus, Y.V., *Nucl. Instrum. Methods Phys. Res., Sect. A*, 2009, vol. 603, p. 95. DOI: 10.1016/j.nima.2008.12.167.
26. Kochubey, D.I., Babanov, Yu.A., Zamaraev, K.I., Vedrinskii, R.V., Kraizman, V.L., Kulipanov, G.N., Mazalov, L.N., Skrinskii, A.N., Fedorov, V.K., Khel'mer, B.Yu., and Shuvaev, A.T., *Rentgenospektral'nyi metod izucheniya struktury amorfnykh tel: EXAFS-spektroskopiya* (X-Ray Spectroscopy for Studying the Structure of Amorphous Materials: EXAFS Spectroscopy), Novosibirsk: Nauka, Sib. Otd., 1988.
27. Newville, M., *J. Synchrotron Radiat*., 2001, vol. 8, p. 96. DOI: 10.1107/S0909049500016290.
28. Zabinski, S.I., Rehr, J.J., Ankudinov, A., and Alber, R.C., *Phys. Rev. B*, 1995, vol. 52, p. 2995. DOI: 10.1103/PhysRevB.52.2995.
29. Allen, F.H., *Acta Crystallogr., Sect. B*, 2002, vol. 58, p. 380. DOI: 10.1107/S0108768102003890.
30. Frisch, M.J., Trucks, G.W., Schlegel, H.B., Scuseria, G.E., Robb, M.A., Cheeseman, J.R., Montgomery, J.A., Jr., Vreven, T., Kudin, K.N., Burant, J.C., Millam, J.M., Iyengar, S.S., Tomasi, J., Barone, V., Mennucci, B., Cossi, M., Scalmani, G., Rega, N., Petersson, G.A., Nakatsuji, H., Hada, M., Ehara, M., Toyota, K., Fukuda, R., Hasegawa, J., Ishida, M., Nakajima, T., Honda, Y., Kitao, O., Nakai, H., Klene, M., Li, X., Knox, J.E., Hratchian, H.P., Cross, J.B., Bakken, V., Adamo, C.,

Jaramillo, J., Gomperts, R., Stratmann, R.E., Yazyev, O., Austin, A.J., Cammi, R., Pomelli, C., Ochterski, J.W., Ayala, P.Y., Morokuma, K., Voth, G.A., Salvador, P., Dannenberg, J.J., Zakrzewski, V.G., Dapprich, S., Daniels, A.D., Strain, M.C., Farkas, O., Malick, D.K., Rabuck, A.D., Raghavachari, K., Foresman, J.B., Ortiz, J.V., Cui, Q., Baboul, A.G., Clifford, S., Cioslowski, J., Stefanov, B.B., Liu, G., Liashenko, A., Piskorz, P., Komaromi, I., Martin, R.L., Fox, D.J., Keith, T., Al-Laham, M.A., Peng, C.Y., Nanayakkara, A., Challacombe, M., Gill, P.M.W., Johnson, B., Chen, W., Wong, M.W., Gonzalez, C., and Pople, J.A., *Gaussian 03,* Revision C 02, Wallingford CT: Gaussian, 2004.

31. Lee, C., Yang, W., and Parr, R.G., *Phys. Rev. B*, 1988, vol. 37, no. 2, p. 785. DOI: 10.1103/PhysRevB.37.785.
32. Becke, A.D., *J. Chem. Phys*., 1993, vol. 98, no. 7, p. 5648. DOI: 10.1063/1.464913.
33. Ditchfield, R., Hehre, W.J., and Pople, J.A., *J. Chem. Phys*., 1971, vol. 54, no. 2, p. 724. DOI: 10.1063/1.1674902.
34. Nivorozhkin, A.L., Toftlund, H., Nivorozhkin, L.E., Kamenetskaya, I.A., Antsishkina, A.S., and Porai-Koshits, M.A., *Transition Met. Chem*., 1994, vol. 19, no. 3, p. 319. DOI: 10.1007/BF00139103.